2017 IEEE International Conference on Robotics and Automation (ICRA)
Singapore, May 29 - June 3, 2017

Extended Tau Theory for Robot Motion Control

Haijie Zhang[1], Bo Cheng[2], and Jianguo Zhao[1]

Abstract— **Biologists proposed the tau theory to explain how animals control their motion using visual feedback for different tasks including landing and perching. Tau theory is based on a concept called time-to-contact, which is the required time to contact an object if the current velocity is maintained. Recently, tau theory has been applied to control robots' motion for similar tasks such as perching, docking, braking, or landing. However, existing tau theory can only work for the case with zero contact velocity. Some tasks such as perching actually require a non-zero contact velocity to make gripping mechanisms work. To address this problem, we extend the tau theory by proposing a two-stage strategy in one dimensional space to generate the reference trajectory for time-to-contact. Moreover, we propose a new coupling strategy to deal with the motion in three dimensional space. Simulation results demonstrate the effectiveness of proposed two-stage and coupling strategies. Moreover, we leverage a featureless method to estimate the time-to-contact from image sequences and implement it on a mobile robot platform. Experimental results also demonstrate that the non-zero contact velocity can be accomplished using onboard vision feedback. The research presented in this paper can be readily applied to control the motion of flying robots for perching with visual feedback.**

I. INTRODUCTION

In biological world, various insects and animals rely on vision to control their motion to interact with uncertain environments [1]. In fact, they can derive the so-called time-to-contact, also known as tau, from consecutive images. Many experiments have shown that tau information is crucial to guide animals' movements: bees have been discovered to keep a constant rate of image expansion during the landing process which is same with constant time-to-contact [2]. Pigeons also adopt time-to-contact to perch on branches [3]. Fruit flies are also found to leverage the inverse of time-to-contact to control the landing and avoid obstacles [4].

The time-to-contact is part of a broad theory called Tau theory, which originates from Gibson's work in which he relates animals' visual information to the locomotion [1]. Based on Gibson's work, Lee first proposed the time-to-contact in [5]. He argued that drivers employed the time-to-contact, rather than distance or speed, to determine when to brake to avoid collision, and time-to-contact could be measured from angular velocities perceived by eyes. In 1998, Lee extended tau theory by introducing tau-coupling [6], which could be used to synchronize movements. The details of tau theory are summarized in [7] and [8].

Recently, there is an increasing trend to apply tau theory to the planning and control of robotic landing, perching, and docking. Souhila *et al.* estimated time-to-contact from optic flow to navigate a mobile robot in cluttered indoor environments [9]. Kaneta *et al.* employed time-to-contact to avoid obstacles and chase another mobile robot [10]. McCarthy *et al.* utilized time-to-contact to control the docking of a mobile robot in front of a vertical wall [11]. Kendoul proposed several time-to-contact controllers to control a quadcopter to realize the docking, landing, and navigation [12], of which the time-to-contact is estimated from GPS. To achieve safe landings, Izzo and Croon proposed different time-to-contact control methods [13]. They estimated time-to-contact from optical flow divergence and validated their control algorithm using a Parrot AR drone [14].

Except Kendoul's experiment, all the time-to-contact is estimated using image sequences from camera. For the image based time-to-contact estimation, there are three widely used methods: size based method [10], [15], optical flow divergence based method [13], [14], [16] and featureless direct method [17], [18]. A common disadvantage of the first two methods is that they need to extract and track features for estimation. As a result, it is not suitable for real-time control, especially for small robots with limited computation power. The third method, which only uses the light intensity of each pixel in the image, is feature independent. We have shown that this method has the potential to be applied to real-time robot control [19] [20].

However, all the tau theory based applications require the contact velocities to be zero, which is not always desired for some robotic perching situations such as [21], [22]. In fact, some perching mechanisms require a substantial velocity (1 m/s) in the direction perpendicular to the object to make sure gripping mechanisms can attach to the object [23], [24]. In such cases with non-zero contact velocity, existing tau theory will not work. To address this problem, we extend the tau theory by proposing a two-stage strategy. Moreover, we propose a new tau-coupling strategy to make the extended theory work in three-dimensional case.

There are two main contributions in this paper. First, we extend the tau theory to realize nonzero contact velocity in both one-dimensional and three-dimensional situations. Such an extension can lead to a more general varying tau-dot strategy [25] as opposed to existing constant tau-dot method. Second, we adopt the featureless tau estimation algorithm to control the robot's motion using image feedback. Such a method can be implemented on miniature robots with limited

*This work is partially supported by the National Science Foundation under Grant CNS-1320561.

[1]Haijie Zhang and Jianguo Zhao are with Department of Mechanical Engineering, Colorado State University, Fort Collins, CO 80523, USA. zhanghaijason@gmail.com, Jianguo.Zhao@colostate.edu

[2]Bo Cheng is with Department of Mechanical and Nuclear Engineering, Pennsylvania State University, University Park, PA 16802, USA buc10@psu.edu

computation power for real-time control.

The rest of this paper is organized as follows. Section II introduces the general tau theory and our extension. Section III describes the featureless tau estimation algorithm and tau controller. To validate the extension of tau theory, section IV details the simulation results for three-dimensional case and experiment for one-dimensional case.

II. Extended Tau Theory for Trajectory Generation

In this section, for the case with non-zero contact velocities, we introduce the extended tau theory for trajectory generation in one dimensional space and a new tau-coupling strategy in three dimensional space.

Suppose t_f is the time when contact occurs, X is the distance gap, and α is the desired contact velocity, then the non-zero contact velocity requirement is

$$\dot{X}(t_f) = \alpha \tag{1}$$

A. General Tau Theory

Before we introduce the extended tau theory, we first briefly review the general tau theory. For the distance gap $X(t)$, tau or time-to-closure/collision/contact (TTC) is defined as:

$$\tau(t) = \frac{X(t)}{\dot{X}(t)} \tag{2}$$

where $\dot{X}(t)$ is the closure rate of the gap. For braking or perching problem, it has been shown that constant tau-dot ($\dot{\tau}$) strategy is adopted by the animals to decelerate to a goal with zero contact velocity [26], [27]. Moreover, comprehensive experiments using robots have been conducted to show the effectiveness of constant tau-dot strategy [12].

For constant tau-dot strategy, we have:

$$\tau(t) = kt + \tau_0, \quad \tau_0 = \frac{X(0)}{\dot{X}(0)} < 0 \tag{3}$$

where k is a constant value for tau-dot. τ_0, $X(0) < 0$, and $\dot{X}(0) > 0$ are the initial conditions. Combining Eqs. (2) and (3), we can solve it for $X(t)$, $\dot{X}(t)$ and $\ddot{X}(t)$:

$$X(t) = X_0(1 + k\frac{\dot{X}_0}{X_0}t)^{1/k} \tag{4}$$

$$\dot{X}(t) = \dot{X}_0(1 + k\frac{\dot{X}_0}{X_0}t)^{1/k-1} \tag{5}$$

$$\ddot{X}(t) = \frac{\dot{X}_0^2}{X_0}(1-k)(1 + k\frac{\dot{X}_0}{X_0}t)^{1/k-2} \tag{6}$$

where $X_0 = X(0)$ and $\dot{X}_0 = \dot{X}(0)$. From analyzing the above equations, we know that only when $0 < k \leq 0.5$, X, $\dot{X}$ and $\ddot{X}$ will become zero at the same finite time. And $\tau(t)$ will also become zero at the same time [12].

However, for the requirement of non-zero contact velocity in Eq. (1), the tau theory will not work. From the equations above, we can in fact show that when the robot achieves the desired velocity α at time t_f, the distance $X(t_f)$ is not zero, which means the robot cannot perch on the desired object.

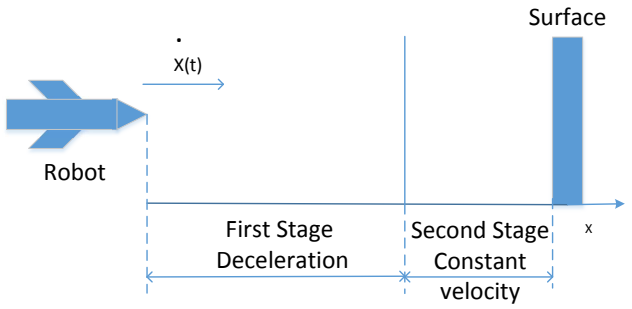

Fig. 1. Sketch for two-stage motion strategy

B. Trajectory Generation in a 1D Space

To generate a trajectory satisfying the requirement in Eq. (1), we divide the whole process into two stages: deceleration stage using constant tau-dot strategy to achieve the desired velocity α and constant velocity stage to close the distance gap. The strategy is illustrated in Fig. 1

Let the duration for the two stages be t_1 and t_2, respectively. Then $t_f = t_1 + t_2$. We are interested in finding the optimal k such that the total time $t_f = t_1 + t_2$ is minimized to realize the fastest motion. The total time for the whole process can be written as:

$$t_f = t_1 + t_2 = \frac{X_0}{k\dot{X}_0}[\beta^{\frac{k}{1-k}} - 1] - \frac{X_0}{\alpha}\beta^{\frac{1}{1-k}} \tag{7}$$

We can show that t_f as a function of $k \in (0,1)$ is monotonically decreasing by showing that the derivative of t_f with respect to k is always negative: $dt_f/dk < 0$. In fact,

$$\frac{dt_f}{dk} = \frac{\beta^{k-1}}{k\alpha}\frac{(k-1)(1-\beta^{\frac{k}{k-1}}) + k\ln\beta}{k(k-1)} \tag{8}$$

Since $\frac{\beta^{k-1}}{k\alpha} > 0$ and $k(k-1) < 0$, we only need to show

$$f(k) = (k-1)(1-\beta^{\frac{k}{k-1}}) + k\ln\beta > 0 \tag{9}$$

for any $k \in (0,1)$. This can be easily proved by obtaining the first order and second order derivative of $f(k)$ with respect to k. Therefore, Eq. (8) is always negative for $k \in (0,1)$, and the total time for the whole process is monotonically decreasing for $k \in (0,1)$. Consequently, we should set $k \to 1$ to achieve fastest motion.

However, k cannot be arbitrarily close to one due to the acceleration constraint for robots, i.e., a robot's acceleration is limited by its motors' capabilities. Let the maximum allowable acceleration be $\ddot{X}_{max}$, then we can obtain the constraint for k. To obtain the maximum deceleration during the fist stage, from Eq. (6), we solve the time derivative for the deceleration:

$$\dddot{X}(t) = (1-2k)(1-k)\frac{\dot{X}_0^3}{X_0^2}(1 + k\frac{\dot{X}_0}{X_0}t)\frac{1-3k}{k} \tag{10}$$

After analysis, we know that when $t \in (0, t_1)$:

- If $0.5 < k < 1$, $\ddot{X}(t)$ will monotonically decrease. Since $\ddot{X}(t) < 0$, so the maximum deceleration should be achieved at $t = t_1$;
- If $0 < k < 0.5$, $\ddot{X}(t)$ will monotonically increase. Since $\ddot{X}(t) < 0$, so the maximum deceleration should be achieved at $t = 0$.

Therefore, the selection of k should respect the following deceleration constraint:

$$\ddot{X}(t_1) = (1-k)\frac{\dot{X}_0^2}{X_0}\left(\frac{\alpha}{\dot{X}_0}\right)^{\frac{1-2k}{1-k}} < \ddot{X}_{max}, \text{ if } 0.5 < k < 1 \quad (11)$$

$$\ddot{X}(0) = (1-k)\frac{\dot{X}_0^2}{X_0} < \ddot{X}_{max}, \text{ if } 0 < k \leq 0.5 \quad (12)$$

In general, to realize the fastest process with a desired contact velocity, a two-stage strategy comprised of a constant tau-dot deceleration stage and a constant velocity stage can be optimal, of which the tau-dot should be selected the largest k which satisfies Eq. (11) or Eq. (12). Therefore, the reference trajectory should be

$$\tau_{ref} = \begin{cases} kt + \tau_0, & \text{if } 0 < t < t_1 \\ \dfrac{X_0 - X(t_1)}{\alpha} + t - t_1, & \text{if } t \geq t_1 \end{cases} \quad (13)$$

C. Trajectory Generation in 3D Space

For trajectory generation in 3D space, the target point is three-dimensional rather than one-dimensional. In this case, for a specific point, we need to close three gaps, namely $X(t)$, $Y(t)$, and $Z(t)$. In tau theory, tau-coupling strategy is used to close several gaps such as angle and distance simultaneously. The tau-coupling strategy states that two gaps X and Y can be synchronized, if the taus of these two gaps are kept in a constant ratio h:

$$\tau_y = h\tau_x \quad (14)$$

where τ_y and τ_x are the taus in Y and X direction, respectively It has been shown that if $0 < h < 0.5$, when $X(t)$ approaches zero, $Y(t)$, $\dot{Y}(t)$ and $\ddot{Y}(t)$ will approach zero at the same time. This can be proved by obtaining the trajectory for $Y(t)$ which is a function of $X(t)$ and some constant parameters determined by the initial conditions.

For our two-stage strategy, we propose a new tau-coupling strategy for the first stage that can both satisfy the non-zero contact velocity requirement and ensure that the gaps of X and Y will close simultaneously. Note that the second stage does not require the coupling since the velocity will be constants in all directions. In order to solve for $Y(t)$ from tau-coupling equation [6], the new tau-coupling strategy for the first stage of the whole process is proposed as:

$$\tau_y = \frac{\tau_x}{b\tau_x + h} \quad (15)$$

where h and b are constants. Integrating Eq. (15), we can get the equations of $Y(t)$, $\dot{Y}(t)$ and $\ddot{Y}(t)$ for the first stage:

$$Y(t) = aX(t)^h e^{bt} \quad (16)$$

$$\dot{Y}(t) = aX(t)^{h-1}e^{bt}(h\dot{X}(t) + bX(t)) \quad (17)$$

$$\begin{aligned}\ddot{Y}(t) = aX(t)^{h-2}e^{bt}[&(h-1)(h\dot{X}(t) + bX(t)) \\ &+X(t)(bh\dot{X}(t) + b^2X(t) + h\ddot{X}(t) + b\dot{X}(t))]\end{aligned} \quad (18)$$

where a is a constant satisfying the initial condition in integration. To make the gaps in X and Y close simultaneously, we need to make sure the time for second stage in two directions are equal, i.e., the following two items should equal:

$$t_{2x} = \frac{X(t_1)}{\dot{X}(t_1)}, \quad t_{2y} = \frac{Y(t_1)}{\dot{Y}(t_1)}$$

From the Eqs. (16) and (17), we can get:

$$t_{2y} = \frac{X(t_1)}{h\dot{X}(t_1) + bX(t_1)} \quad (19)$$

Therefore, to make $t_{2y} = t_{2x}$, we can solve the constant b:

$$b = \frac{(1-h)\dot{X}(t_1)}{X(t_1)} \quad (20)$$

Similarly, to close the gap in Z direction at the same time, another tau-coupling law $\tau_z = \dfrac{\tau_x}{b_z\tau_x + h_z}$ can be used, where b_z, h_z are constants similar to b and h.

III. Featureless Time-to-contact Estimation and Control

From Eqs. (13) and (15), we have the trajectory for reference taus. To control the actual tau to the reference value, we need to estimate tau for feedback. For humans and animals, tau can be perceived by eyes, while for robots, it can be estimated from GPS or cameras. Since GPS or distance sensor might be heavy and large for small size robots, we are interested in estimating tau from image sequences. Specifically, we employ a featureless estimation algorithm which does not need feature extraction and tracking [17]. There are four cases for this algorithm, but we only introduce the robustest one in which the optical axis of camera attached to a robot is perpendicular to the object or surface and moving along an arbitrary straight direction towards the object or surface.

In this case, let three linear velocities for the robot be: $\dot{X}(t)$, $\dot{Y}(t)$, $\dot{Z}(t)$, and the X axis of the camera frame is perpendicular to the surface. Then time-to-contact in X direction, namely $\dfrac{X(t)}{\dot{X}(t)}$ can be estimated from Eq. (21):

$$\begin{bmatrix} \sum I_x^2 & \sum I_x I_y & \sum G I_x \\ \sum I_x I_y & \sum I_y^2 & \sum G I_y \\ \sum G I_x & \sum G I_y & \sum G^2 \end{bmatrix} \begin{bmatrix} A \\ B \\ C \end{bmatrix} = - \begin{bmatrix} \sum I_x I_t \\ \sum I_y I_t \\ \sum G I_t \end{bmatrix} \quad (21)$$

where $A = -\frac{\dot{Y}(t)}{\dot{X}(t)}$, $B = -\frac{\dot{Z}(t)}{\dot{X}(t)}$, $C = \frac{\dot{X}(t)}{\dot{X}(t)}$, I is the light intensity of a pixel on the image, I_x, I_y are the derivatives of I with respect to x, y direction of the image frame respectively, I_t is the derivative of I with respect to time and $G = xI_x + yI_y$. And $\sum$ is an abbreviation of $\sum_{i=1}^{m}\sum_{j=1}^{n}$, where i, j are the pixel index in an $m \times n$ image. The accuracy and computational speed of this method are detailed in [20].

With the tau feedback from camera, we can control the time-to-contact to track the reference trajectory. The

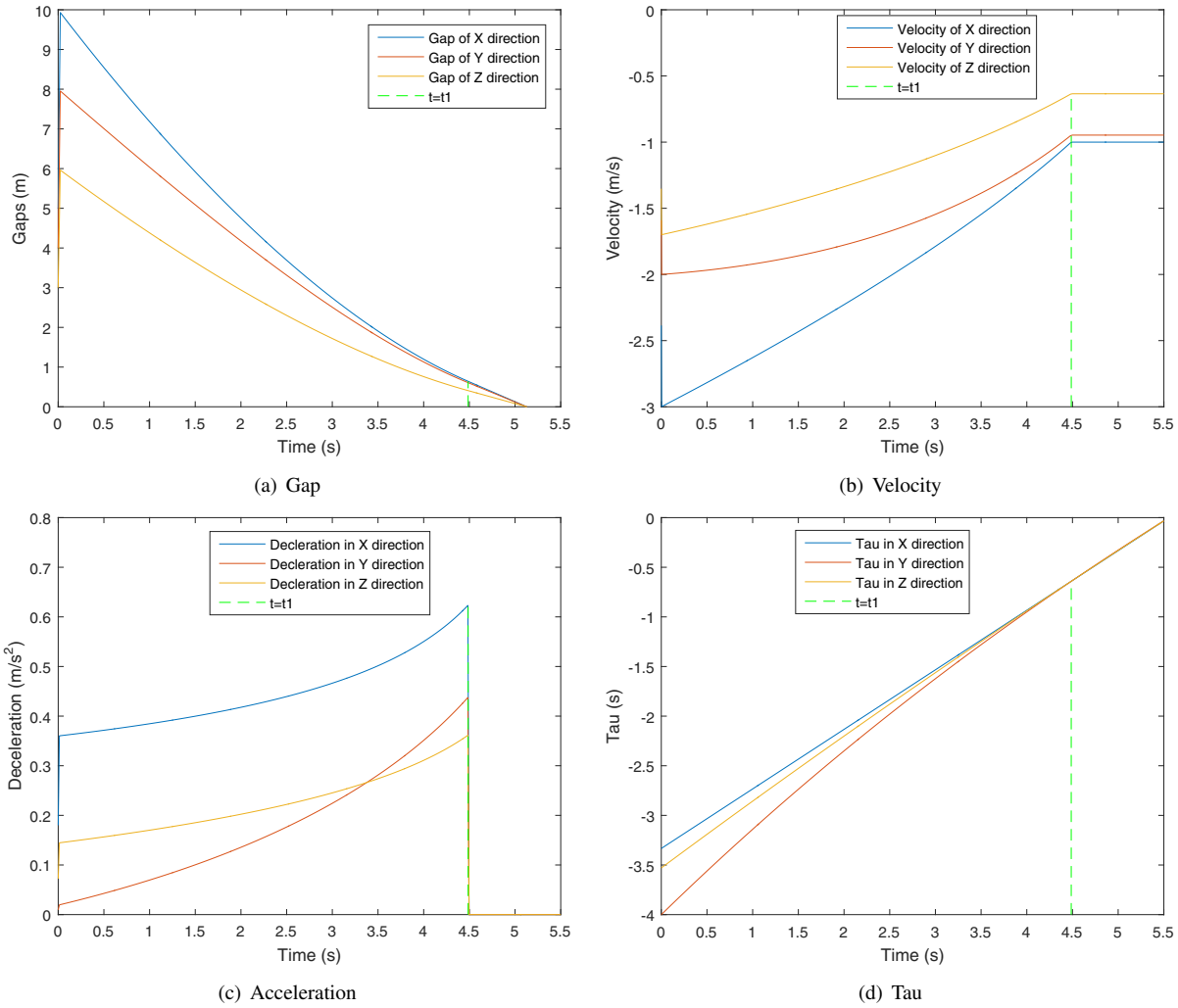

(a) Gap (b) Velocity

(c) Acceleration (d) Tau

Fig. 2. Simulation result for gap, velocity, acceleration and tau respectively under the two-stage strategy and the new tau-coupling strategy.

reference tau is shown in Eq. (13) for one dimensional case. In [19], we have proposed an error based proportional controller and shown its advantages compared with a standard fixed gain proportional controller. The error based proportional controller is

$$V_{i+1} = \begin{cases} K_1(\tau - \tau_{ref}) + V_i, & \text{if } \tau - \tau_{ref} > 0 \\ K_2(\tau - \tau_{ref}) + V_i, & \text{if } \tau - \tau_{ref} < 0 \end{cases} \tag{22}$$

where $K_1 > 0$ and $K_2 > 0$ are the proportional gains, V_i is the current velocity, and V_{i+1} is the next desired velocity.

IV. Simulation and Experiment Results

In this section, we first simulate the robot motion under the two-stage strategy and new tau-coupling strategy to show three gaps can be closed simultaneously and the requirement of non-zero contact velocity can be fulfilled. Then we conduct the two-stage strategy experiment with a mobile robot platform using the tau feedback from distance sensor and image, respectively, to show that the two-stage strategy has the potential to be applied for robot motion control.

A. Simulation Results

For the new tau-coupling strategy, we set the initial conditions as: $X_0 = 10m$, $\dot{X}_0 = -3m/s$, $\alpha = -1m/s$, $\ddot{X}(t)_{max} = 0.7m/s^2$, $Y_0 = 8m$, $\dot{Y}_0 = -2m/s$, $Z_0 = 6m$, $\dot{Z}_0 = -1.7m/s$. According to the maximum acceleration constraint, we set $k = 0.6$. From these conditions, we can solve $t_1 = 4.4864s$. With the two-stage strategy and new tau-coupling strategy, the gap, velocity, deceleration, and tau in X, Y, and Z directions are shown in Fig. 2.

In Fig. 2, the blue lines represent the gap, velocity, acceleration and tau in X direction. It shows that the two-stage strategy can satisfy the requirements in Eq. (1), the gap will be closed, the velocity will decrease to $-1m/s$ then keep constant, the acceleration will not be a large number, and tau will approach zero finally. Compared with the blue lines, the red and yellow lines represent the gap, velocity, acceleration and tau in Y and Z direction, respectively. And it shows that the new tau-coupling strategy can be used to close several gaps simultaneously. Thus, the simulation results demonstrate that both the two-stage strategy and the new tau-coupling strategy can be used for non-zero contact

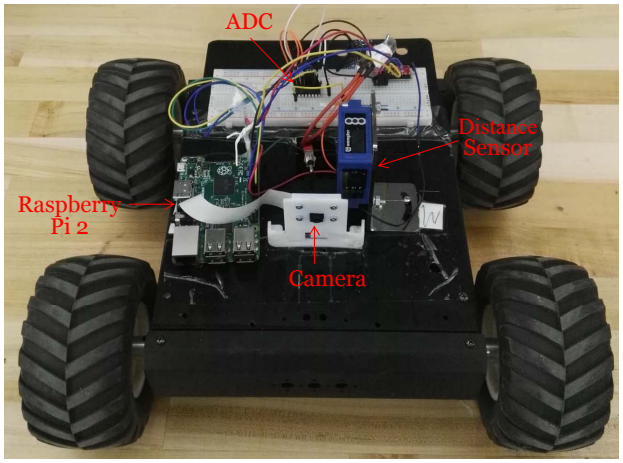

Fig. 3. Mobile robot platform

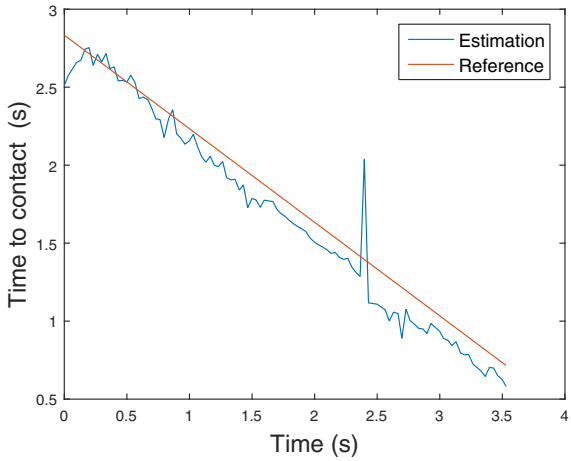

(a) Estimated time-to-contact

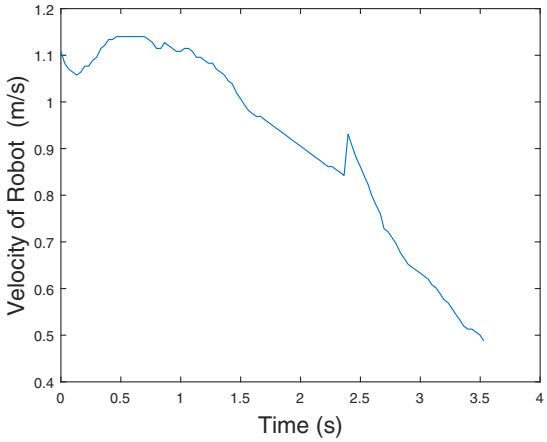

(b) Speed of robot

Fig. 4. Experiment results for distance sensor based tau feedback

velocity tasks.

B. Experiment results for two-stage strategy

For this experiment, we conduct docking experiments using a mobile robot platform facing a vertical wall. The goal is to control the robot's motion with the two-stage strategy so that non-zero contact velocity can be achieved. Two experiments are performed with the tau feedback estimated from a distance sensor and a camera, respectively.

An integrated system in Fig. 3 is developed for onboard docking control. A mobile robot (A4WD1 from Robotshop) serves as the main platform. A Raspberry Pi 2 is used as the central processing unit to interface with a camera, estimate the time-to-contact, and compute the control command. An Arduino board (Arduino Pro 328 from Sparkfun) is employed to achieve closed-loop speed control of the robot. A Raspberry Pi camera and distance sensor (OPT 2011 from Autodirect) are fixed on top of the robot and facing forward. An ADC chip (Mcp3008 from Sparkfun) is used for the Raspberry Pi 2 to read the distance data. Several papers with checkerboard patterns are randomly placed on a wall that the robot will move towards.

For both experiments, the robot starts with an initial velocity of 1.14m/s, an initial distance 3.2m, $k = 0.6$, a desired contact velocity $\alpha = 0.475m/s$. Note that in both distance sensor based experiment and image based experiment, when the robot decelerates to α, to avoid possible collisions with the wall, we stop the robot and measure the distance from the robot to the wall. To see the performance of the strategy, we compare the measured distance with the theoretical distance when robot decelerates to α. According to the two-stage strategy, the final distance from the robot to the wall should be 0.36m. Fig. 4 shows the experiment results using the tau feedback (sampling frequency ∼35Hz) calculated from the ratio between distance (from distance sensor) and velocity (from encoder feedback) with a final distance of 0.247m. Fig. 5 shows the experiments result using the tau feedback (sampling frequency ∼20Hz) from image sequences, with a final distance of 0.75m.

From Fig. 4, we can see that even though there are errors caused by the distance sensor, the estimated time-to-contact almost follows the reference time-to-contact. When the time-to-contact is larger than the reference value, the controller will increase the speed to decrease time-to-contact. On the other hand, when the time-to-contact is less than the reference value, the controller will decrease the speed to increase time-to-contact. From Fig. 5, the estimated time-to-contact can also follow the trend of the reference, but there are larger errors. The errors may be caused by the camera quality and small angular velocities caused by uneven ground. The experiment results show that the two-stage strategy can be applied to the robot motion control such as perching, docking and braking tasks with the non-zero contact velocity requirements.

V. Conclusions

Tau theory has been widely applied for robot motion control for tasks such as landing and docking. In this paper, we extend the tau theory to deal with the non-zero contact velocity. Specifically, we propose a two-stage strategy and a new tau-coupling strategy to make sure that the non-zero

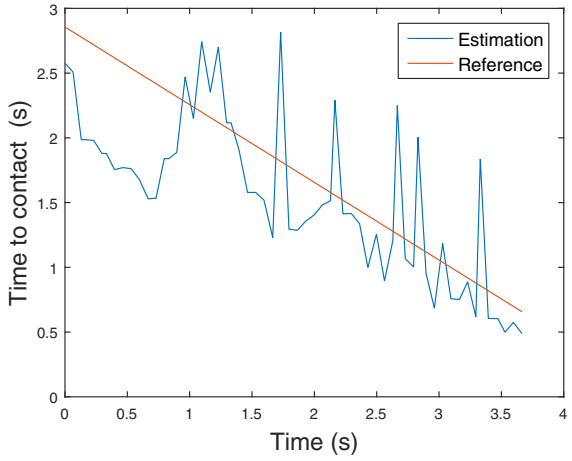

(a) Estimated time-to-contact

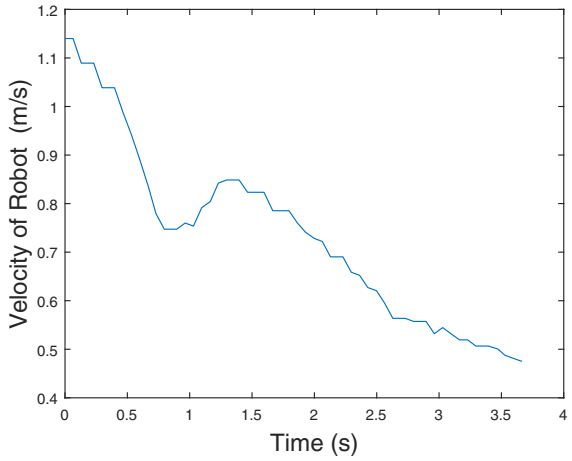

(b) Speed of robot

Fig. 5. Experiment results for image based tau feedback

contact velocity can be accomplished. Simulations demonstrate the effectiveness of the proposed strategies. Moreover, experiments with a mobile robot for one dimensional motion with a distance sensor for feedback also validate the two-stage strategy. In addition, experiments with a camera for feedback demonstrate that onboard vision based control using the two-stage strategy is possible. In the future, we will implement the two-stage strategy and new coupling strategy in three-dimensional space with a flying robot using onboard vision feedback.

REFERENCES

[1] J. J. Gibson, "Visually controlled locomotion and visual orientation in animals," *British journal of psychology*, vol. 49, no. 3, pp. 182–194, 1958.

[2] E. Baird, N. Boeddeker, M. R. Ibbotson, and M. V. Srinivasan, "A universal strategy for visually guided landing," *Proceedings of the National Academy of Sciences*, vol. 110, no. 46, pp. 18686–18691, 2013.

[3] D. N. Lee, M. N. Davies, P. R. Green, *et al.*, "Visual control of velocity of approach by pigeons when landing," *Journal of Experimental Biology*, vol. 180, no. 1, pp. 85–104, 1993.

[4] F. Van Breugel and M. H. Dickinson, "The visual control of landing and obstacle avoidance in the fruit fly drosophila melanogaster," *Journal of Experimental Biology*, vol. 215, no. 11, pp. 1783–1798, 2012.

[5] D. N. Lee, "A theory of visual control of braking based on information about time-to-collision," *Perception*, vol. 5, no. 4, pp. 437–459, 1976.

[6] D. N. Lee, "Guiding movement by coupling taus," *Ecological psychology*, vol. 10, no. 3-4, pp. 221–250, 1998.

[7] D. N. Lee, "General tau theory: evolution to date.," *Perception*, vol. 38, no. 6, p. 837, 2009.

[8] D. N. Lee, "Tau in action in development," in *Action As An Organizer of Learning and Development: Volume 33 in the Minnesota Symposium on Child Psychology Series*, vol. 33, p. 1, Psychology Press, 2016.

[9] K. Souhila and A. Karim, "Optical flow based robot obstacle avoidance," *International Journal of Advanced Robotic Systems*, vol. 4, no. 1, pp. 13–16, 2007.

[10] Y. Kaneta, Y. Hagisaka, and K. Ito, "Determination of time to contact and application to timing control of mobile robot," in *Robotics and Biomimetics (ROBIO), 2010 IEEE International Conference on*, pp. 161–166, IEEE, 2010.

[11] C. McCarthy, N. Barnes, and R. Mahony, "A robust docking strategy for a mobile robot using flow field divergence," *IEEE Transactions on Robotics*, vol. 24, no. 4, pp. 832–842, 2008.

[12] F. Kendoul, "Four-dimensional guidance and control of movement using time-to-contact: Application to automated docking and landing of unmanned rotorcraft systems," *The International Journal of Robotics Research*, vol. 33, no. 2, pp. 237–267, 2014.

[13] D. Izzo and G. D. Croon, "Landing with time-to-contact and ventral optic flow estimates," *Journal of Guidance, Control, and Dynamics*, vol. 35, no. 4, pp. 1362–1367, 2012.

[14] G. De Croon, H. Ho, C. De Wagter, E. Van Kampen, B. Remes, and Q. Chu, "Optic-flow based slope estimation for autonomous landing," *International Journal of Micro Air Vehicles*, vol. 5, no. 4, pp. 287–298, 2013.

[15] G. de Croon, D. Izzo, and G. Schiavone, "Time-to-contact estimation in landing scenarios using feature scales," *Acta Futura*, vol. 5, pp. 73–82, 2012.

[16] T. Camus, "Calculating time-to-contact using real-time quantized optical flow," *National Institute of Standards and Technology NISTIR*, vol. 5609, p. 51, 1995.

[17] B. K. Horn, Y. Fang, and I. Masaki, "Hierarchical framework for direct gradient-based time-to-contact estimation," in *IEEE Intelligent Vehicles Symposium*, pp. 1394–1400, 2009.

[18] B. K. Horn, Y. Fang, and I. Masaki, "Time to contact relative to a planar surface," in *IEEE intelligent vehicles symposium*, pp. 68–74, 2007.

[19] H. Zhang and J. Zhao, "Biologically inspired vision based control using featureless time-to-contact estimations," in *Advanced Intelligent Mechatronics (AIM), 2016 IEEE International Conference on*, pp. 1133–1138, IEEE, 2016.

[20] H. Zhang and J. Zhao, "Bio-inspired vision based robot control using featureless estimations of time-to-contact," *Bioinspiration & Biomimetics*, vol. 12, no. 2, p. 025001, 2017.

[21] J. Thomas, M. Pope, G. Loianno, E. W. Hawkes, M. A. Estrada, H. Jiang, M. R. Cutkosky, and V. Kumar, "Aggressive flight with quadrotors for perching on inclined surfaces," *Journal of Mechanisms and Robotics*, vol. 8, no. 5, p. 051007, 2016.

[22] J. Moore, R. Cory, and R. Tedrake, "Robust post-stall perching with a simple fixed-wing glider using lqr-trees," *Bioinspiration & biomimetics*, vol. 9, no. 2, p. 025013, 2014.

[23] C. E. Doyle, J. J. Bird, T. A. Isom, J. C. Kallman, D. F. Bareiss, D. J. Dunlop, R. J. King, J. J. Abbott, and M. A. Minor, "An avian-inspired passive mechanism for quadrotor perching," *IEEE/ASME Transactions on Mechatronics*, vol. 18, no. 2, pp. 506–517, 2013.

[24] L. Daler, A. Klaptocz, A. Briod, M. Sitti, and D. Floreano, "A perching mechanism for flying robots using a fibre-based adhesive," in *Robotics and Automation (ICRA), 2013 IEEE International Conference on*, pp. 4433–4438, IEEE, 2013.

[25] W. Chi, K. H. Low, and K. H. Hoon, "A fuzzy control strategy for uav perching using varying tau-dot," in *AIAA Guidance, Navigation, and Control Conference*, p. 0891, 2016.

[26] D. N. Lee, P. E. Reddish, and D. Rand, "Aerial docking by hummingbirds," *Naturwissenschaften*, vol. 78, no. 11, pp. 526–527, 1991.

[27] D. N. Lee, J. A. Simmons, P. A. Saillant, and F. Bouffard, "Steering by echolocation: a paradigm of ecological acoustics," *Journal of Comparative Physiology A*, vol. 176, no. 3, pp. 347–354, 1995.